Available online at www.sciencedirect.com
ScienceDirect
Journal of Sound and Vibration 305 (2007) 808–826
JOURNAL OF SOUND AND VIBRATION
www.elsevier.com/locate/jsvi

The buckling of functionally graded truncated conical shells under dynamic axial loading

A.H. Sofiyev*

Department of Civil Engineering of Suleyman Demirel University, Isparta, Turkey

Received 16 October 2006; received in revised form 1 May 2007; accepted 1 May 2007
Available online 27 June 2007

Abstract

The dynamic buckling of truncated conical shells made of functionally graded materials (FGMs) subject to a uniform axial compressive load, which is a linear function of time, has been studied. The material properties of functionally graded shells are assumed to vary continuously through the thickness of the shell. The variation of properties followed an arbitrary distribution in terms of the volume fractions of the constituents. The fundamental relations, the dynamic stability and compatibility equations of functionally graded truncated conical shells are obtained first. Applying Galerkin's method, these equations have been transformed to a pair of time dependent differential equation with variable coefficient and critical parameters obtained using the Runge–Kutta method. The results show that the critical parameters are affected by the configurations of the constituent materials, compositional profile variations, loading speed variations and the variation of the shell geometry. Comparing the results of this study with those in the literature validates the present analysis.

1. Introduction

Functionally graded materials (FGMs) are composite materials with gradient compositional variation of the constituents (e.g. metallic and ceramic) from one surface of the material to the other that results in continuously varying material properties. The concept of FGM [1], initially developed for super heat resistant materials to be used in space planes or nuclear fusion reactors, is now of interest to designers of functional materials for energy conversion [2], dental and orthopedic implants [3], sensors and thermo-generators [4]. FGMs are also used for joining dissimilar materials [5]. A general account of FGMs, including fabrication and characterization of properties, is given in Suresh and Mortensen [5] and Miyamoto et al. [6].

The stability and vibration behaviors of FGM shell structures have attracted increasing research effort, most of which have been limited to the vibration analysis. A formulation of the stability problem for functionally graded hybrid composite plates, where a micro mechanical model was employed to solve the buckling problem for rectangular plates subjected to uniaxial compression presented by Birman [7]. Loy et al. [8] studied the vibration of stainless steel and nickel graded cylindrical shells under simply supported ends by using Love's theory and Rayleigh–Ritz method. Pradhan et al. [9] presented the vibration of a functionally graded cylindrical shell. The effects of boundary condition and volume fractions on the natural frequencies

*Tel.: +90 246 2111195; fax: +90 246 2370859.
E-mail address: asofiyev@mmf.sdu.edu.tr

0022-460X/$ - see front matter © 2007 Elsevier Ltd. All rights reserved.
doi:10.1016/j.jsv.2007.05.002

Nomenclature

e_s, e_θ, $e_{s\theta}$ Strain components on the reference surface of the conical shell
E Young's modulus of the FG conical shell
E_{0t}, E_{0b} Young's moduli of purely ceramic and metal conical shells, respectively
E_t, E_b Young's moduli of the ceramic and metal surfaces of the FG conical shell, respectively
$f_1(t)$, $\bar{f}_1(t)$ amplitude and dimensionless amplitude parameter, respectively
F stress function
h thickness of the conical shell
L length of the conical shell
m_s, m_θ, $m_{s\theta}$ moment resultants
n_s, n_θ, $n_{s\theta}$ force resultants
$n_s^0, n_\theta^0, n_{s\theta}^0$ membrane forces prior to buckling
n, m wavenumbers
$n_{cr}^{st}; n_{cr}^{din}$ circumferential wavenumbers corresponding to critical static and dynamic axial loads, respectively
N, N_0 static axial load and axial loading speed, respectively
N_{cr}^{st}, $\bar{N}_{cr}^{st}$ critical static axial load and critical dimensionless static axial load, respectively
P, P_j $(j=-1$ to $3)$ material properties
P_t, P_b material properties of the top and bottom surfaces of the conical shell, respectively
Q_{ij} reduced stiffness
R_1, R_2 average radii of the small and large bases of the conical shell
S coordinate axis through the vertex on the reference surface of the cone
S_1, S_2 inclined distances of the bases of the cone from the vertex, respectively
$t_{cr}, \bar{t}_{cr}$ critical time and critical dimensionless time parameter, respectively
T temperature in Kelvin
V_c, V_m volume fractions of ceramic and metal surfaces, respectively
w displacement of the reference surface in the inwards normal direction z
$\bar{z} = z/h$ dimensionless thickness coordinate
θ angle of rotation around the longitudinal axis starting from a radial plane
v Poisson's ratio of the FG conical shell
v_t, v_b Poisson's ratios of the ceramics and metal surfaces of the FG conical shell, respectively
v_{0t}, v_{0b} Poisson's ratios of purely ceramic and metal conical shells, respectively
ρ_1 density of the FGM conical shell
ρ_t, ρ_b densities of ceramic and metal surfaces of the FG conical shell, respectively
ρ_{0t}, ρ_{0b} densities of purely ceramic and metal conical shells, respectively
σ_s, σ_θ, $\sigma_{s\theta}$ stress components
σ^{cr} critical static axial stress
ξ independent variable
ζ coordinate axis in the inwards normal direction of the reference surface of the cone

were studied. Reddy and Cheng [10] established the exact correspondences between the vibration frequencies of membranes and FGM spherical shallow shells. A self-consistent constitutive framework is proposed to describe the behavior of a generic three-layered system containing a FGM layer subjected to thermal loading given by Pitakthapanaphong and Busso [11]. Woo and Meguid [12] studied the post-buckling behaviors of functionally graded plates and shallow shells under transverse mechanical loads and temperature field. Yang and Shen [13] studied parametric resonance of shear deformable functionally graded cylindrical panels in thermal environment. Shen [14] presented a post-buckling analysis for a functionally graded cylindrical thin shell of finite length subjected to external pressure and in thermal environments. Kitipornchai et al. [15] further evaluated the sensitivity of the nonlinear vibration characteristics of FGM plates to the initial geometric imperfection of arbitrary shape. Chen et al. [16] investigated free vibration of a functionally graded piezoelectric hollow cylinder filled with a compressible fluid medium. Based on the high order shear deformation theory, Patel et al. [17] gave the finite element analysis for the free vibration of FGM elliptical cylindrical shell. Liew et al. [18] presented the nonlinear vibration analysis for layered cylindrical panels containing FGMs and subjected to a temperature gradient arising from steady heat conduction through the panel thickness. A finite element formulation based on FSDT is used to study the thermal buckling and vibration behavior of truncated FGM conical shells in a high-temperature environment and presented by

Bhangale et al. [19]. Bhangale and Ganesan [20] studied free vibration anisotropic and linear magneto-electro-elastic FG plates have been carried out semi-analytical finite element method.

The buckling of conical shells is of fundamental interest in aircraft and missile design as thin-walled shells have constituted primary structural parts for many years, and because the composite materials are nowadays extremely attractive due to their considerable strength-to-weight ratio. They are subjected to various loading both static and dynamic. Studies of static buckling of conical shells under axial load have received its due importance in the literature [21–31].

It is well known, due to the difficulties emerging from the solution and theoretical analysis of the stability problems of shells, such as suddenly applied loads, has not been studied sufficiently. So it is important to study the dynamic stability behavior of conical shells under suddenly applied loads. It is known that, the researchers use two concepts in the solution of the dynamic stability problems. A relatively well-defined class of dynamic stability problems is the dynamic buckling behavior under step loading or impulsive loading. There are different criteria for the solution of the buckling problems. For example: Simitises and Budiansky–Roth criteria [32–35].

Another important class of dynamic stability problems is the buckling behavior under a-periodic dynamic loading. This concept is based on the assumption that, the stress and the deformation occurring in different points of the deformable body under the effect of dynamic load, may suddenly propagate to whole volume of the body. When the equation of the motion of the system (shell) element is constituted, an inertia force corresponding to the normal displacement is taken into consideration. Consequently, in this state, propagation of elastic waves in the middle surface was not taken into consideration. The solution of a dynamic stability problem is reduced to the determination of the dynamic critical load or critical time for certain loading cases. In the literature, one may find many criteria allowing for determination of dynamic critical loads. One of the important criterion was proposed by Volmir [36] where the dynamic critical load corresponds to the amplitude of force (of constant duration) at which the maximum shell defection is equal to some constant value k (k-one half or one shell thickness). Pioneering papers on dynamic buckling of conical shells subjected to a-periodic dynamic axial loads were written by Wolmir [36] and Shumik [37]. In recent years, the buckling problems of the homogeneous and non-homogeneous orthotropic conical shells under a-periodic dynamic external pressure were also extensively studied in Refs. [38–42].

Researches on the dynamic stability of FGM plates and shells subjected to various loads by using different methods and criterions are limited. Praveen and Reddy [43] analyzed the nonlinear static and dynamic response of heated functionally graded ceramic-metal plates subjected to dynamic lateral loads by the finite element method. Reddy and Chin [44] presented thermal-mechanical analysis of functionally graded cylinders and plates. Reddy [45] developed both theoretical and finite element formulations for thick FGM plates according to the higher-order shear deformation plate theory, and studied the nonlinear dynamic response of FGM plates subjected to sudden applied uniform pressure. Ng et al. [46] studied the parametric resonance or dynamic stability of FGM cylindrical thin shells under periodic axial loading. Yang and Shen [47] studied the dynamic response of initially stressed FG rectangular thin plates subjected to partially distributed impulsive lateral loads and without or resting on an elastic foundation. To achieve the active control of the static and dynamic response of FGM shells, Liew et al. [48], He et al. [49] and Ng et al. [50] used the piezoelectric materials as the integrated sensors/actuators. Vel and Batra [51] analyzed forced vibrations of simply supported functionally graded plates and their response to time-dependant thermal loads (within the context of uncoupled quasi-static linear thermo-elasticity theory) using the power series method. By using Galerkin technique together with Ritz type variational method, Sofiyev and Schnack [52] and Sofiyev [53,54] obtained critical parameters for cylindrical thin shells under a linearly increasing dynamic torsional loading, for functionally graded truncated conical shells under a-periodic external pressure and for cylindrical shells under axial compressive load, which is a power function of time. Kubiak [55] studied the dynamic response of a thin walled plate with varying widthwise material properties subjected to in-plane pulse loading of rectangular shape. Budiansky–Hutchinson criterion of dynamic stability was chosen to determine the critical value of dynamic load factor. Tylikowski [56] studied the dynamic stability of the FG plates subjected time-dependent, in plane forces, using the direct Liapunov method and asymptotic stability criteria. Zhu et al. [57] presented a three-dimensional theoretical analysis of the dynamic instability region of functionally graded (FG) piezoelectric circular cylindrical shells. A set of Mathieu–Hill equations governing the instability problem is derived and analyzed by Bolotin's method. Wu et al. [58] investigated the dynamic stability of thick FGM plates

subjected to aero-thermo-mechanical loads, using a novel numerical solution technique, the moving least squares differential quadrature method. Ganapathi [59] studied the dynamic stability behavior of a clamped FGMs spherical shell structural element subjected to external pressure load. He solved the governing equations employing the Newmark's integration technique coupled with a modified Newton–Raphson iteration scheme.

The dynamic buckling problems of composite truncated conical shells that composed of FGM subjected to compressive load depending of time have not been studied yet. Therefore, it is very important to develop an accurate, reliable analysis towards the understanding of the dynamic buckling characteristics of the FGM structures.

In this paper, the dynamic buckling of functionally graded truncated conical shells subjected to axial compressive load varying as a linear function of time is studied by using Galerkin and Runge–Kutta methods, and applying criterion proposed by Wolmir [36]. Extensive numerical results are presented in dimensionless tabular forms to demonstrate the influence of material compositions, loading speed, as well as the shell geometry on the critical dimensionless static axial load and critical dimensionless time parameter values. The numerical results are validated against known data in the literature.

2. Analytical model of FGM material properties

A truncated conical shell made of FGM is shown in Fig. 1, where R_1 and R_2 indicate the radii of the cone at its small and large ends, respectively, γ denotes the semi-vertex angle of the cone, H is height of truncated conical shell, L is length of truncated conical shell, S axis lies along the generator on the curvilinear reference surface of the cone, the θ axis lies in the circumferential direction on the reference surface of the cone and the z axis, being perpendicular to the plane of the first two axes, lies in the inwards normal direction of the cone, and the distances from the vertex to the small and large bases are S_1 and S_2, respectively.

Here we consider an FGM shell made of a mixture of ceramics and metals. We assume that the composition is varied from the top to bottom surface, i.e. the top surface ($z = h/2$) of the shell is ceramic-rich whereas the bottom surface ($z = -h/2$) is metal-rich. In such a way, the effective material properties P, like Young's modulus E or Poisson's ratio v or mass density ρ, can be expressed as

$$P = P_t V_c + P_b V_m, \tag{1}$$

where P_t and P_b denote the temperature-dependent properties of the top and bottom surfaces of the shell, respectively; V_c and V_m are the ceramic and metal volume fractions and the related by

$$V_c + V_m = 1. \tag{2}$$

The compositional gradation of the FGM shell is defined by the volume fraction of the ceramic phase. Here, the following functions of V_c will be considered [11]:

$$\text{1. Linear :} \qquad V_c = \bar{z} + 0.5 \tag{3.1}$$

$$\text{2. Quadratic :} \qquad V_c = (\bar{z} + 0.5)^2 \tag{3.2}$$

$$\text{3. Inverse quadratic :} \qquad V_c = 1 - (0.5 - \bar{z})^2 \tag{3.3}$$

$$\text{4. Cubic :} \qquad V_c = 3(\bar{z} + 0.5)^2 - 2(\bar{z} + 0.5)^3, \tag{3.4}$$

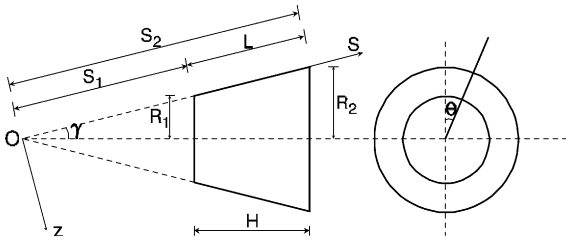

Fig. 1. The geometry and coordinate system of a truncated conical shell.

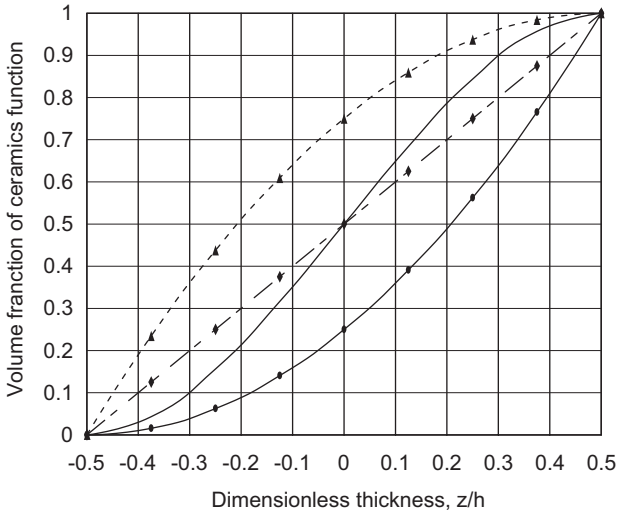

Fig. 2. Different composition profiles used to describe the variation of ceramic volume fraction in the FGM conical shell (dashed line with diamonds = linear; solid line with circles = quadratic; dashed line with triangles = inverse quadratic; bold solid line = cubic).

where $\bar{z} = z/h$ is dimensionless thickness coordinate. The variation of the ceramic volume fraction through the thickness of FG shell is shown in Fig. 2. The vertical-axis stands for the volumetric percentage of ceramic while horizontal-axis represents the position along the thickness of FG shell. Metal is the dominant constituent at the bottom layer of FG shell and its volume fraction is decreased continually from the bottom to the top of FG shell. At the top layer of FG shell, ceramic is the dominant constituent.

From Eqs. (1)–(3), the effective Young's modulus E, Poisson ratio v and the mass density ρ, of an FGM shell can be written as

$$E = (E_t - E_b)V_c + E_b, \quad v = (v_t - v_b)V_c + v_b, \quad \rho = (\rho_t - \rho_b)V_c + \rho_b. \tag{4}$$

It is assumed that E_t, E_b, v_t, v_b, ρ_t and ρ_b are the Young's modulus, Poisson's ratio and density of the metal and ceramic surfaces of the FG conical shell, respectively and are the functions of temperature, as shown in Section 4, so that E, v and ρ are functions of temperature and position.

From these equations the followings are obtained:

$$\begin{cases} E = E_t, \quad v = v_t, \quad \rho = \rho_t, \quad \text{at} \quad \bar{z} = 0.5, \\ E = E_b, \quad v = v_b, \quad \rho = \rho_b, \quad \text{at} \quad \bar{z} = -0.5. \end{cases} \tag{5}$$

Therefore, the material properties along the thickness of the shells, such as Young's modulus E, Poisson's ratio v can be determined according to Eq. (4).

3. The governing equations

With the help of these material properties, the stress–strain relations for thin conical shells can be determined as

$$\begin{bmatrix} \sigma_s \\ \sigma_\theta \\ \sigma_{s\theta} \end{bmatrix} = \begin{bmatrix} Q_{11} & Q_{12} & 0 \\ Q_{12} & Q_{22} & 0 \\ 0 & 0 & Q_{66} \end{bmatrix} \begin{bmatrix} e_s - \dfrac{\partial^2 w}{\partial s^2} \\ e_\theta - \dfrac{1}{s^2}\dfrac{\partial^2 w}{\partial \varphi^2} - \dfrac{1}{s}\dfrac{\partial w}{\partial s} \\ e_{s\theta} - \dfrac{1}{s}\dfrac{\partial^2 w}{\partial s \partial \varphi} + \dfrac{1}{s^2}\dfrac{\partial w}{\partial \varphi} \end{bmatrix}, \tag{6}$$

where $\varphi = \theta \sin\gamma$, σ_S, σ_θ and $\sigma_{S\theta}$ are the stresses components, e_S, e_θ and $e_{S\theta}$ are the strains components on the reference surface, w is the displacement of the reference surface in the normal direction, positive towards the axis of the cone and assumed to be much smaller than the thickness and Q_{ij} $(i, j = 1, 2, 6)$ are defined as

$$Q_{11} = Q_{22} = \frac{(E_t - E_b)V_c + E_b}{1 - [(v_t - v_b)V_c + v_b]^2}, \tag{7}$$

$$Q_{12} = \frac{[(E_t - E_b)V_c + E_b][(v_t - v_b)V_c + v_b]}{1 - [(v_t - v_b)V_c + v_b]^2}, \tag{8}$$

$$Q_{66} = \frac{(E_t - E_b)V_c + E_b}{2[1 + (v_t - v_b)V_c + v_b]} \tag{9}$$

The following integrals define the stress and moment resultants:

$$(n_s, n_\theta, n_{s\theta}) = h\int_{-0.5}^{0.5} (\sigma_s, \sigma_\theta, \sigma_{s\theta})\,\mathrm{d}\bar{z}, \qquad (m_s, m_\theta, m_{s\theta}) = h^2\int_{-0.5}^{0.5} (\sigma_s, \sigma_\theta, \sigma_{s\theta})\bar{z}\,\mathrm{d}\bar{z}. \tag{10}$$

Introducing an Airy stress function F, the force resultants $(n_s, n_\theta, n_{s\theta})$ are given as follows:

$$(n_s, n_\theta, n_{s\theta}) = \left(\frac{1}{s^2}\frac{\partial^2 F}{\partial\varphi^2} + \frac{1}{s}\frac{\partial F}{\partial s}, \quad \frac{\partial^2 F}{\partial s^2}, \quad -\frac{1}{s}\frac{\partial^2 F}{\partial s\partial\varphi} + \frac{1}{s^2}\frac{\partial F}{\partial\varphi}\right). \tag{11}$$

According to the membrane theory of shells, the dynamic stability and strain compatibility equations are given in the following form with loading terms in the coefficients of the derivatives of displacement w:

$$\begin{aligned}&\frac{\partial^2 m_s}{\partial s^2} + \frac{2}{s}\frac{\partial m_s}{\partial s} + \frac{2}{s}\frac{\partial^2 m_s\theta}{\partial s\partial\varphi} - \frac{1}{s}\frac{\partial m_\theta}{\partial s} + \frac{2}{s^2}\frac{\partial m_{s\theta}}{\partial\varphi} + \frac{1}{s^2}\frac{\partial m_{s\theta}}{\partial\varphi^2} + \frac{n_\theta}{s}\cot\gamma\\ &\quad + n_s^0\frac{\partial^2 w}{\partial s^2} + \frac{n_\theta^0}{s}\left(\frac{1}{s}\frac{\partial^2 w}{\partial\varphi^2} + \frac{\partial w}{\partial s}\right) + 2n_{s\theta}^0\frac{\partial}{\partial s}\left(\frac{1}{s}\frac{\partial w}{\partial\varphi}\right) - \rho_1 h\frac{\partial^2 w}{\partial t^2} = 0,\end{aligned} \tag{12}$$

$$\frac{\cot\gamma}{s}\frac{\partial^2 w}{\partial s^2} - \frac{2}{s}\frac{\partial^2 e_{s\theta}}{\partial s\partial\varphi} - \frac{2}{s^2}\frac{\partial e_{s\theta}}{\partial\varphi} + \frac{\partial^2 e_\theta}{\partial s^2} + \frac{1}{s^2}\frac{\partial^2 e_s}{\partial\varphi^2} + \frac{2}{s}\frac{\partial e_\theta}{\partial s} - \frac{1}{s}\frac{\partial e_s}{\partial s} = 0, \tag{13}$$

where the following definition applies:

$$\rho_1 = \int_{-0.5}^{0.5} \left[(\rho_t - \rho_b)V_c + \rho_b\right]\mathrm{d}\bar{z}. \tag{14}$$

The functionally graded conical shell subjected to axial compressive load varying as a linear function of time in the form:

$$n_S^0 = -N - N_0 t, \tag{15}$$

where N_0 is the axial loading speed, N is the static axial load and t is the time.

Substituting the constitutive law (6), Eqs. (10), (11) and (15) into Eqs. (12) and (13), then considering the independent variables $s = s_1 e^{\xi}$ and $F = F_1 e^{2\xi}$, the dynamic stability and strain compatibility equations of FG

conical shells can be reduced to

$$
\begin{aligned}
&A_2e^{2\xi}\frac{\partial^4F_1}{\partial\xi^4}+4A_2e^{2\xi}\frac{\partial^3F_1}{\partial\xi^3}+\left(4A_2+s_1e^{\xi}\cot\gamma\right)e^{2\xi}\frac{\partial^2F_1}{\partial\xi^2}\\
&+3s_1\cot\gamma e^{2\xi}\frac{\partial F_1}{\partial\xi}+2s_1\cot\gamma e^{2\xi}F_1+A_2e^{2\xi}\frac{\partial^4F_1}{\partial\varphi^4}+2(A_1-A_5)e^{2\xi}\frac{\partial^4F_1}{\partial\xi^2\partial\varphi^2}\\
&+4(A_1-A_5)e^{2\xi}\frac{\partial^3F_1}{\partial\xi\partial\varphi^2}+2(A_1-A_5+A_2)e^{2\xi}\frac{\partial^2F_1}{\partial\varphi^2}\\
&-A_3\frac{\partial^4w}{\partial\varphi^4}-2(A_4+A_6)\frac{\partial^4w}{\partial\xi^2\partial\varphi^2}+4(A_4+A_6)\frac{\partial^3w}{\partial\xi\partial\varphi^2}-2(A_4+A_6+A_3)\frac{\partial^2w}{\partial\varphi^2}\\
&-A_3\frac{\partial^4w}{\partial\xi^4}+4A_3\frac{\partial^3w}{\partial\xi^3}-4A_3\frac{\partial^2w}{\partial\xi^2}-s_1^2e^{2\xi}(N+N_0t)\left(-\frac{\partial w}{\partial\xi}+\frac{\partial^2w}{\partial\xi^2}\right)-\rho_1hs_1^4e^{4\xi}\frac{\partial^2w}{\partial t^2}=0,
\end{aligned}
\tag{16}
$$

$$
\begin{aligned}
&B_1\left(\frac{\partial^4F_1}{\partial\xi^4}+4\frac{\partial^3F_1}{\partial\xi^3}+4\frac{\partial^2F_1}{\partial\xi^2}+\frac{\partial^4F_1}{\partial\varphi^4}\right)+2(B_5+B_2)\left(\frac{\partial^4F_1}{\partial\xi^2\partial\varphi^2}+2\frac{\partial^3F_1}{\partial\xi\partial\varphi^2}\right)+2(B_5+B_2+B_1)\frac{\partial^2F_1}{\partial\varphi^2}\\
&=e^{-2\xi}\left[\begin{array}{c}B_4\dfrac{\partial^4w}{\partial\varphi^4}+2(B_3-B_6)\dfrac{\partial^4w}{\partial\xi^2\varphi^2}+4(B_6-B_3)\dfrac{\partial^3w}{\partial\xi\partial\varphi^2}+2(B_3+B_4-B_6)\dfrac{\partial^2w}{\partial\varphi^2}\\ +B_4\dfrac{\partial^4w}{\partial\xi^4}-4B_4\dfrac{\partial^3w}{\partial\xi^3}+\left(4B_4-s_1e^{\xi}\cot\gamma\right)\dfrac{\partial^2w}{\partial\xi^2}+s_1e^{\xi}\cot\gamma\dfrac{\partial w}{\partial\xi}\end{array}\right],
\end{aligned}
\tag{17}
$$

where expressions A_i, B_i ($i=1$–6) are given in Appendix (A.1–A.14).

Eqs. (16) and (17) are the basic equations for dynamic stability of FG conical shells subjected to dynamic axial compressive load.

4. The solution of governing equations

Considering a truncated conical shell with simply supported edge conditions, the solutions for Eq. (17) take the following form [40]:

$$w=f_1(t)e^{\xi}\sin\beta_1\xi\sin\beta_2\varphi \tag{18}$$

where $f_1(t)$ is time dependent amplitude and the following definitions apply:

$$\beta_1=\frac{m\pi}{\xi_0},\quad \beta_2=\frac{n}{\sin\gamma},\quad \xi_0=\ln\frac{s_2}{s_1},\quad \xi=\ln\frac{s}{s_1}. \tag{19}$$

Function (18) satisfies the periodical conditions of the normal displacements and all orders of the derivatives for normal displacements and the following geometrical boundary conditions Lu and Chung [60] and Agamirov [40]:

$$w=0,\qquad \text{at}\quad \xi=0\quad\text{and}\quad \xi=\xi_0, \tag{20}$$

$$\frac{\partial^2w}{\partial\xi^2}-\frac{\partial w}{\partial\xi}=0,\qquad \text{at}\quad \xi=0\quad\text{and}\quad \xi=\xi_0. \tag{21}$$

Substituting Eq. (18) into Eq. (17) and by applying the superposition principle the particular solution to resultant equation, can be obtained as

$$F_1=(K_1\sin\beta_1\xi+K_2\cos\beta_1\xi+K_3e^{-\xi}\sin\beta_1\xi)f_1(t)\sin\beta_2\varphi \tag{22}$$

where the following definitions apply:

$$K_1=\frac{\beta_1(\beta_1\psi_0+\psi_2)}{\psi_0^2+\psi_2^2}s_1\cot\gamma,\quad K_2=\frac{\beta_1(\beta_1\psi_2-\psi_0)}{\psi_0^2+\psi_2^2}s_1\cot\gamma,\quad K_3=\frac{\psi_3}{\psi_1}, \tag{23}$$

where

$$\psi_0 = B_1(\beta_2^4 - 3\beta_1^2) + 2(B_5 + B_2)\beta_1^2\beta_2^2 - 2(B_5 + B_2 + B_1)\beta_2^2,$$
$$\psi_1 = 2(B_5 + B_2)\beta_1^2\beta_2^2 + B_1(\beta_1^4 + \beta_2^4 + 2\beta_1^2 - 2\beta_2^2 + 1),$$
$$\psi_2 = 4B_1\beta_1^3 + 4(B_5 + B_2)\beta_1\beta_2^2,$$
$$\psi_3 = B_4\left[\left(\beta_2^2 - 1\right)^2 + \beta_1^2\right] + \beta_1^2\left[2(B_3 - B_6)\beta_2^2 + B_4(\beta_1^2 + 1)\right]. \tag{24}$$

Substituting Eqs. (18) and (22) into Eq. (16), then applying Galerkin's method in the ranges $0 \leqslant \varphi \leqslant 2\pi \sin\gamma$ and $0 \leqslant \xi \leqslant \xi_0$, after integrating the following equation is obtained:

$$\frac{d^2 f_1(t)}{dt^2} + \frac{q_9}{\rho_1 h q_8}\left[\frac{U_1 q_1 + U_2 q_2 + U_3 q_3 + q_7}{q_9} - (N + N_0 t)\right] f_1(t) = 0, \tag{25}$$

where the following definitions apply:

$$U_1 = A_2(K_1\beta_1^4 + 4K_2\beta_1^3 - 4K_1\beta_1^2 + K_1\beta_2^4 - 2K_1\beta_2^2) + 2\beta_2^2(K_1\beta_1^2 + 2K_2\beta_1 - K_1)(A_1 - A_5) - K_3\beta_1^2 s_1 \cot\gamma, \tag{26.1}$$

$$U_2 = A_2(K_3\beta_1^4 + 2K_3\beta_1^2 + K_3 + K_3\beta_2^4 - 2K_3\beta_2^2) + 2K_3\beta_1^2\beta_2^2(A_1 - A_5) - A_3(\beta_1^4 + 2\beta_1^2 + \beta_2^4 - 2\beta_2^2 + 1) - 2\beta_1^2\beta_2^2(A_6 + A_4), \tag{26.2}$$

$$U_3 = A_2(K_2\beta_1^4 - 4K_1\beta_1^3 - 4K_2\beta_1^2 + K_2\beta_2^4 - 2K_2\beta_2^2) - 2\beta_2^2(A_1 - A_5)(K_2\beta_1^2 + 2K_1\beta_1 + K_2) + K_3\beta_1 s_1 \cot\gamma, \tag{26.3}$$

$$q_1 = \frac{2\beta_1^2\left(1 - e^{3\xi_0}\right)}{\left(12\beta_1^2 + 27\right)}, \quad q_2 = \frac{\beta_1^2\left(1 - e^{2\xi_0}\right)}{4\left(\beta_1^2 + 1\right)}, \quad q_3 = \frac{\beta_1\left(e^{3\xi_0} - 1\right)}{4\beta_1^2 + 9},$$
$$q_4 = \frac{\beta_1^2(1 - e^{4\xi_0})}{8\left(\beta_1^2 + 4\right)}, \quad q_5 = \frac{\beta_1\left(e^{4\xi_0} - 1\right)}{4(\beta_1^2 + 4)}, \quad q_6 = \frac{\beta_1^2\left(e^{6\xi_0} - 1\right)}{12\left(\beta_1^2 + 9\right)},$$
$$q_7 = \left[(-3K_2\beta_1 - K_1\beta_1^2 + 2K_1)q_4 - (K_2\beta_1^2 - 3K_1\beta_1 - 2K_2)q_5\right] s_1 \cot\gamma$$
$$q_8 = s_1^4 q_6, \quad q_9 = s_1^2\beta_1(q_5 - \beta_1 q_4). \tag{27.1)–(27.9}$$

At static case, for the critical dimensionless axial load, the following expression is obtained:

$$\bar{N}_{cr}^{st} = \frac{N_{cr}^{st}}{E_{0t} h}, \tag{28}$$

where E_{0t} is Young's modulus of the homogeneous ceramic and the following definition apply:

$$N_{cr}^{st} = \frac{U_1 q_1 + U_2 q_2 + U_3 q_3 + q_7}{q_9}. \tag{29}$$

The classical critical static axial load for a truncated conical shell made of a homogeneous isotropic material was found by Seide [24]:

$$N_{Seide}^{cr} = \frac{2\pi E_0 h^2 \cos^2\gamma}{\sqrt{3(1 - \nu_0^2)}}. \tag{30}$$

When $n_s^0 = 0$, the following expression is obtained from Eq. (25) for the frequency of free vibration:

$$\omega = \sqrt{\frac{U_1 q_1 + U_2 q_2 + U_3 q_3 + q_7}{q_9 \rho_1 h}}. \tag{31}$$

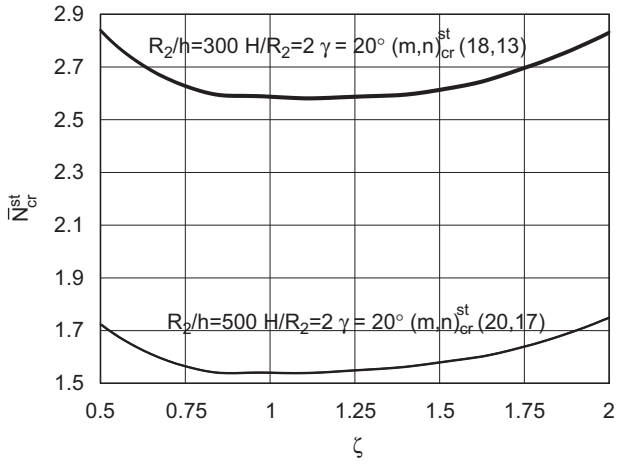

Fig. 3. Variations of the values of critical dimensionless static axial load $\bar{N}_{cr}^{st}$ corresponding to ζ.

When $n_s^0 = N_0 t$, from Eq. (25), the following dimensionless equation is expressed:

$$\frac{d^2\bar{f}_1(t)}{d\bar{t}^2} + Q[1-\bar{t}]\bar{f}_1(t) = 0, \tag{32}$$

where $\bar{f}_1(t)$ is dimensionless amplitude parameter, $\bar{t}$ is dimensionless time parameter and the following definitions apply:

$$Q = \frac{3}{2} \times \frac{h^2\left[\bar{N}_{cr}^{st}(\zeta)\right]^3 E_{0t}^3}{N_0^2\rho_1} \frac{\zeta^2 + 9/\beta_2^2}{\zeta^2 + 4/\beta_2^2} \frac{s_1^2 + s_2^2}{s_1^4 + s_1^2 s_2^2 + s_2^4} (2/\beta_2^2 + \zeta^2)\beta_2^2,$$
$$\zeta = \frac{\beta_1}{\beta_2}, \quad \bar{t} = \frac{N_0 t}{\bar{N}_{cr}^{st}(\zeta) E_{0t} h}, \quad \bar{f}_1 = \frac{f_1}{h}. \tag{33}$$

Firstly, minimizing the expression (29) according to the wavenumbers (m, n), the minimum values of critical dimensionless static axial load are obtained. Then, substituting placing the relation $\zeta = \beta_1/\beta_2$ into the expression (29) to be used for dynamic problem, the relation $\bar{N}_{cr}^{st}(\zeta)$ is formed. At $0.1 \leqslant \zeta \leqslant 2$, the smallest value of the minimum values of the critical dimensionless static axial load corresponding to circumferential wavenumber is numerically obtained approximately for $\zeta = 1$ (Fig. 3). Furthermore, it is shown that the values obtained from the minimization of the static critical load according to the wavenumbers (m, n) are coincided with the values obtained from the minimization of the static critical load according to the parameters (ζ, n).

Then the numerical solution of the dynamic problem is obtained.

Eq. (32) is solved numerically by using Runge–Kutta method with the following initial conditions:

$$\bar{t} = 0, \quad \bar{f}_1 = \bar{f}_{10}, \quad d\bar{f}_1/d\bar{t} = 0. \tag{34}$$

Solution of Eq. (32) explains a time dependent monotonously increasing function. Furthermore, the amplitude initially increases slowly but it indicates an instantaneous increase later. The case for the equality of the amplitude to the shell thickness (beginning of the strong increase for amplitude) corresponds to the beginning of the loss of stability and is assumed as the stability criterion. Using this criterion $\bar{t}_{cr}$ is found for variable loading speeds [36].

5. Numerical results and discussion

5.1. Comparison results

The numerical results are compared with the previous works to demonstrate the performance of the present study.

Firstly, results that are obtained from present study for values of critical static axial load of isotropic conical shell are compared with the results of Seide [24]. After transforming the expression (30) obtained for conical shell in Seide [24] and the expression (29) obtained in present study to the following expressions, computations are made:

$$\sigma_{\text{Seide}}^{\text{cr}} = \frac{N_{\text{Seide}}^{\text{cr}}}{2\pi R_m h \cos\gamma}, \tag{35}$$

$$\sigma_{\text{Sofi}}^{\text{cr}} = \frac{N_{\text{cr}}^{\text{st}}}{h}. \tag{36}$$

Computations have been carried out for the following material and shell properties are: $E = 2.1 \times 10^5$ MPa; $v = 0.3$; $L = 0.25R_2 \sin\gamma$; $R_2/h = 400$; $R_m = (R_1 + R_2)/2$; $h = 0.0005$ m. It shows that the results are very convenient (Table 1).

To verify the present analysis, the buckling loads for cylindrical shells under axial compression are calculated and compared in Table 2 with the Donnell-type shell theory solution of Jones and Morgan [61], with the boundary layer theory solution of Shen [62], and Shen and Li [63]. To be able to make comparisons with cylindrical shells, in expression (29) $\gamma = \pi/180000 \approx 0^\circ$ must be substituted for the semi-vertex angle and so $R_2 \approx R_1 \approx R$ must be assumed. The comparisons for the shell with the following material properties [61]: $E_1 = 30 \times 10^6$ psi; $E_2 = 0.75 \times 10^6$ psi; $G_{12} = 0.375 \times 10^6$ psi; $v_1 = 0.25$; $v_2 = 0.0625$, $h = 0.12$ in; $R_1 = R = 10$ in; $L = 34.64$ in; $\gamma = \pi/180\,000$ are presented in Table 2. The comparisons show that the present result is in good agreement with that the results of Jones and Morgan [61], Shen [62], and Shen and Li [63].

To further verify the present analysis, natural vibration frequency is compared with the FG shell in literature (see Table 3). Computations are made for the natural frequency of FG circular cylindrical shell using expression (31), and the results are compared with those of Loy et al. [8]. To be able to make comparisons with FG cylindrical shells, in expression (31) $\gamma = \pi/180\,000 \approx 0^\circ$ must be substituted for the semi-vertex angle and so $R_2 \approx R_1 \approx R$ must be assumed. In Table 3, first and last columns are the natural frequency values of homogeneous stainless steel cylindrical shell, the other columns are the values of the FG cylindrical shell made of stainless steel and nickel. Homogeneous stainless steel material properties are as follows:

Table 1
Comparison of the values of critical static axial stress with those of Seide [24]

σ^{cr} (MPa)				
γ	30°	45°	60°	75°
Seide [24]	284.05	239.66	175.31	93.096
Present study	283.44	238.25	172.52	89.754

Table 2
Comparison of dimensionless axial buckling load for orthotropic cylindrical shell

$N_{\text{cr}}^{\text{st}} L^2/(E_2 h^3)$ and (m, n)			
Jones and Morgan [61]	Shen [62]	Shen and Li [63]	Present study
1482	1481.75 (3, 7)	1481.75 (3, 7)	1481.95 (3, 7)

Table 3
Comparison of natural frequencies (Hz) for simply supported FG circular cylindrical shells with those of Loy et al. [8]

Circum. wave no (n)	$\bar{\omega}=\omega/(2\pi)$ (Hz)					
	Loy et al. [8]			Present study		
	Stain. steel	Linear	Quadratic	Linear	Quadratic	Stain. steel
5	11.542	11.241	11.151	11.935	11.840	12.094
6	16.897	16.455	16.323	17.150	17.018	17.383
7	23.244	22.735	22.635	23.339	23.152	23.648
8	30.573	29.903	29.771	30.447	30.233	30.880
9	38.881	38.028	37.862	38.569	38.260	39.079
10	48.168	46.905	46.529	47.613	47.232	48.242

Table 4
Comparison of the values of critical dimensionless static axial load and of critical dimensionless time parameter with those of Agamirov [40]

R_2/h	γ	Agamirov [40]		Present study		$N_0\times10^{-9}$ (N/m × s)	Agamirov [40]		Present study	
		$\bar{N}_{cr}^{st}\times10^3$	n_{cr}^{st}	$\bar{N}_{cr}^{st}\times10^3$	$(m,n)_{cr}^{st}$		$\bar{t}_{cr}$	n_{cr}^{din}	$\bar{t}_{cr}$	n_{cr}^{din}
500	10°	1.42	19	1.415	(18, 18)	1	3.06	26	3.05	28
						2.5	4.93	33	4.90	31
						5	7.04	40	6.96	42
500	20°	1.56	18	1.551	(20, 17)	1	2.94	24	2.94	25
						2.5	4.72	31	4.70	27
						5	6.81	37	6.56	35

The numbers of buckling waves (m, n) are denoted in parenthesis in present study.

$E_{0t}=2.0104\times10^{11}\,\mathrm{N/m^2}$, $v_{0t}=0.3262$, $\rho_{0t}=8166\,\mathrm{kg/m^3}$. Material properties of FG shell made of stainless steel and nickel are as follows: $h=0.002\,\mathrm{m}$, $R/h=500$, $L/R=20$, $E_t=2.07788\times10^{11}\,\mathrm{N/m^2}$, $v_t=0.317756$, $\rho_t=8166\,\mathrm{kg/m^3}$, $E_b=2.05098\times10^{11}\,\mathrm{N/m^2}$, $v_b=0.31$, $\rho_b=8900\,\mathrm{kg/m^3}$. The comparisons show that the present results for FG shell agreed well with those in the literature.

In addition to validate the analysis, results of critical dimensionless static axial load, critical dimensionless time parameter and dynamic wavenumbers for simply supported homogeneous elastic truncated conical shells are compared with the results of Agamirov [40], see Table 4. Computations have been carried out for the following data:

Material properties $E_0=2.1\times10^5\,\mathrm{MPa}$; $v_0=0.3$.
Shell properties $h=5\times10^{-4}\,\mathrm{m}$; $H/R_2=2$; $\bar{f}_{10}=0.001$.
Velocity of sound in the material $V=5\times10^3\,\mathrm{m/s}$.

The comparisons show that the present results agreed well with those in the literature.

5.2. Buckling results of FG truncated conical shells

The analysis of the FG truncated conical shells was conducted for two types of ceramic and metal combinations. The first set of materials considered was Silicon nitride and Nickel, referred to as Si_3N_4/Ni or FG-I. The second one was a combination of Zirconia and Titanium, referred to as ZrO_2/Ti–6Al–4V or FG-II. The material properties P can be expressed as a function of temperature as

$$P=P_0(P_{-1}T^{-1}+1+P_1T+P_2T^2+P_3T^3), \tag{37}$$

Table 5
Temperature-dependent coefficients of Young's modulus E (MPa), Poisson's ratio v and mass density ρ (kg/m^3) for ceramics and metals (Reddy and Chin [44])

Coefficients	E_t (MPa)	v_t	ρ_t (kg/m^3)	E_b (MPa)	v_b	ρ_b (kg/m^3)
	Si_3N_4			Ni		
P_0	3.4843×10^5	0.24	2370	2.2395×10^5	0.31	8900
P_{-1}	0	0	0	0	0	0
P_1	-3.07×10^{-4}	0	0	-2.794×10^{-4}	0	0
P_2	2.160×10^{-7}	0	0	-3.998×10^{-9}	0	0
P_3	-8.946×10^{-11}	0	0	0	0	0
P	3.2227×10^5	0.24	2370	2.05098×10^5	0.31	8900
	ZrO_2			Ti–6Al–4V		
P_0	2.4427×10^5	0.2882	3000	1.2256×10^5	0.2884	4420
P_{-1}	0	0	0	0	0	0
P_1	-1.371×10^{-3}	1.133×10^{-4}	0	-4.586×10^{-4}	1.121×10^{-4}	0
P_2	1.214×10^{-6}	0	0	0	0	0
P_3	-3.681×10^{-9}	0	0	0	0	0
P	1.68063×10^5	0.298	3000	1.056982×10^5	0.2981	4420

*The properties were evaluated at $T=300$ K.

where P_0, P_{-1}, P_1, P_2 and P_3 are the coefficients of temperature T (K) expressed in Kelvin and are unique to the constituent materials [64]. Typical values for Si_3N_4, Ni, ZrO_2 and Ti–6Al–4V listed in Table 5. In all cases, the upper surface of the conical shell is assumed to be ceramic (Si_3N_4 or ZrO_2) rich and the lower surface is assumed to be pure metal (Ni or Ti–6Al–4V). The materials are assumed to be perfectly elastic throughout the deformation. E_{0t}, E_{0b}, v_{0t}, v_{0b}, ρ_{ot} and ρ_{ob} are the Young's modulus, Poisson's ratio and density of the homogeneous metal and ceramic materials of the shell.

Shells with two different types of geometry are assumed for computation of the critical dimensionless static axial load. In first type shells (A), values of the critical dimensionless static axial load are obtained for $\gamma\leqslant20^\circ$ because of the consideration of the ratio $H/R_2=2$ (see Refs. [40,60]). In second type shells (B), values of the critical dimensionless static axial load are obtained for $\gamma>20^\circ$ because of the consideration of the relation $L=0.25\times R_2\sin\gamma$ (see Ref. [29]). Besides, the values of the longitudinal wavenumber (m) corresponding to the critical static axial load is different from one and larger than the values of the circumferential wavenumber (n) in first type shells (see Table 6). The values of the longitudinal wavenumber (m) corresponding to the critical static axial load are equal one in second type conical shells. Type A conical shells are used in Tables 4 and 6. Type B conical shells are used in Tables 1–3 and 7–9. For FG conical shells, when compositional profile changes linear, quadratic and cubic, and for full metal and ceramic conical shells as the wavenumbers corresponding to the critical dimensionless static axial load are the same. The wavenumbers are shown only in the column for the full ceramic shells.

In Table 7, variations of the values of critical dimensionless static axial load, critical dimensionless time parameter and corresponding wavenumbers for homogeneous and FG-I type and FG-II type conical shells composed of Si_3N_4 /Ni and ZrO_2 /Ti–6Al–4V with different compositional profiles and loading speeds, are presented.

When loading speed N_0 is increased, values of the critical dimensionless time parameter and dynamic wavenumbers are also increased. Wavenumbers corresponding to the dynamic critical axial load is bigger than the wavenumbers corresponding to critical static axial load and when loading speed N_0 is increased, this difference increases more. Furthermore, the values of the critical dimensionless time parameter are very sensitive according to the wavenumbers so they can have instantaneous variations. It is very important for the examination the values of critical dimensionless time parameter.

According to the variations of the loading speed N_0, comparing the values of critical dimensionless time parameter of full ceramic conical shells with the values for FG conical shells, the largest effect (as percent) is

Table 6
Variations of the values of critical dimensionless static axial load for FG-I and FG-II type conical shells with different compositional profiles, R_2/h and γ ($H/R_2 = 2$)

R_2/h	γ	Si_3N_4	Si_3N_4/Ni				Ni
			Linear	Quadratic	Cubic	Inverse quad	
		$\bar{N}_{cr}^{st} \times 10^3$; $(m,n)_{cr}^{st}$					
300	10°	2.317(14, 14)	1.770	1.663	1.763	1.876(18, 12)	1.521
300	15°	2.455(17, 13)	1.875	1.762	1.868	1.988(18, 13)	1.611
300	20°	2.539(17, 13)	1.939	1.822	1.932	2.055(19, 13)	1.666
500	10°	1.391(18, 18)	1.062	0.998	1.058	1.126(21, 17)	0.913
500	15°	1.474(21, 17)	1.125	1.057	1.121	1.194(22, 17)	0.967
500	20°	1.524(21,17)	1.164	1.094	1.160	1.234(22, 17)	1.000
			ZrO_2 /Ti–6Al–4V				
R_2/h	γ	ZrO_2	Linear	Quadratic	Cubic	Inverse quad	Ti–6Al–4V
		$\bar{N}_{cr}^{st} \times 10^3$ $(m,n)_{cr}^{st}$					
300	10°	2.349(14, 14)	1.310	1.229	1.305	1.391(18, 12)	1.179
300	15°	2.489(17, 13)	1.388	1.302	1.382	1.474(19, 12)	1.249
300	20°	2.574(17, 13)	1.435	1.346	1.430	1.524(19, 13)	1.291
500	10°	1.410(18, 18)	0.787	0.738	0.783	0.834(21, 17)	0.707
500	15°	1.494(21, 17)	0.833	0.781	0.830	0.884(22, 17)	0.749
500	20°	1.545(20, 17)	0.862	0.808	0.858	0.915(22, 17)	0.775

observed at quadratic case and the least effect is observed at inverse quadratic case (Note, the following expression is used for percents: [(FG−Hom)/Hom] × 100%). At quadratic case; in FG-I type conical shells, for $N_0 = 1 \times 10^9$; 3×10^9 and 5×10^9 (N/m × s), the effects are 56%, 101.2% and 94%, respectively; in FG-II type conical shells the effects are 72.9%, 80.9% and 61.8%, respectively. At inverse quadratic case; in FG-I type conical shells, for $N_0 = 1 \times 10^9$; 3×10^9 and 5×10^9 (N/m × s) the effects are 29.1%, 49.5% and 63.1%; in FG-II type conical shells the effects are 45.8%, 64.6% and 42.3 %, respectively.

According to the variations of the loading speed N_0, comparing the values of critical dimensionless time parameter of full metal conical shells with the values for FG conical shells, the largest effect is seen at inverse quadratic case and the least effect is seen at quadratic case. At inverse quadratic case; in FG-I type conical shells, for $N_0 = 1 \times 10^9$; 3×10^9 and 5×10^9 (N/m × s) the effects are 29.9%, 33.4% and 25.8%, respectively; in FG-II type conical shells the effects are 23%, 14.1% and 16.3%, respectively. At quadratic case; in FG-I type conical shells, for $N_0 = 1 \times 10^9$; 3×10^9 and 5×10^9 (N/m × s) the effects are 15.3%, 10.4% and 11.8%, respectively; in FG-II type conical shells the effects are 8.7%, 5.6% and 4.8%, respectively.

Comparison of the values of critical dimensionless time parameter for FG-I type and FG-II type conical shells, the values for FG-I type conical shells are seen lower. Furthermore, in FG-I type conical shells; loss of the stability is seen at the small values of the dynamic wavenumbers.

In FG-I and FG-II type conical shells, the values of critical dimensionless time parameter vary between the values for full ceramic and full metal conical shells (see Table 7).

In Table 8, variations of values of critical dimensionless static axial load, critical dimensionless time parameter and corresponding wavenumbers for homogeneous, FG-I type and FG-II type conical shells composed of Si_3N_4/Ni and ZrO_2/Ti–6Al–4V, respectively with different compositional profiles and semi-vertex angle γ are presented.

When semi-vertex angle γ is increased, the values of critical dimensionless static axial load, the wavenumbers corresponding to it and the values of dynamic wavenumbers are also decreased, but the values of the critical dimensionless time parameter is increased.

According to the variations of the semi-vertex angle γ, comparing the values of critical dimensionless time parameter of full ceramic conical shells with the values for FG conical shells, the largest effect is seen at quadratic case and the least effect is seen at inverse quadratic case. At quadratic case; in FG-I type conical

Table 7
Variations of the values of critical dimensionless static axial load, critical dimensionless time parameter and wave numbers for homogeneous, FG-I type and FG-II type conical shells with different compositional profiles and loading speeds N_0 ($R_2/h = 400$; $\gamma = 45^\circ$; $L = 0.25 \times R_2 \sin\gamma$)

$\bar{N}_{cr}^{st} \times 10^3$	$(m,n)_{cr}^{st}$	$\bar{N}_{cr}^{st} \times 10^3$	$(m,n)_{cr}^{st}$	$N_0 \times 10^{-9}$ (N/m × s)	$\bar{t}_{cr}$	n_{cr}^{din}	$\bar{t}_{cr}$	n_{cr}^{din}
Si_3N_4/Ni								
Linear		Quadratic			Linear		Quadratic	
0.851	(1, 15)	0.800	(1, 15)	1	3.290	17	3.628	17
				3	5.904	21	6.801	22
				5	7.443	26	7.784	26
Cubic		Inverse quad.			Cubic		Inverse quad.	
0.848	(1, 15)	0.902	(1, 15)	1	3.299	17	3.003	17
				3	5.932	21	5.055	21
				5	7.442	26	6.546	26
Si_3N_4		Ni			Si_3N_4		Ni	
1.114	(1, 15)	0.732	(1, 15)	1	2.326	17	4.284	17
				3	3.381	21	7.592	22
				5	4.013	26	8.824	26
ZrO_2 /Ti–6Al–4V								
Linear		Quadratic			Linear		Quadratic	
0.630	(1, 15)	0.591	(1, 15)	1	4.613	21	5.046	21
				3	7.812	28	8.252	28
				5	9.068	34	9.699	34
Cubic		Inverse quad.			Cubic		Inverse quad.	
0.627	(1, 15)	0.668	(1, 15)	1	4.636	21	4.257	21
				3	7.834	28	7.509	28
				5	9.102	34	8.531	34
ZrO_2		Ti–6Al–4V			ZrO_2		Ti–6Al–4V	
1.130	(1, 15)	0.567	(1, 15)	1	2.919	18	5.528	21
				3	4.561	24	8.741	28
				5	5.996	28	10.19	35

shells, for $\gamma = 30^\circ; 45^\circ; 60^\circ$ the effects are 48.5%, 60% and 77.2%, respectively; in FG-II type conical shells the effects are 53%, 72.9% and 97.5%, respectively. At inverse quadratic case, in FG-I type conical shells, for $\gamma = 30^\circ, 45^\circ, 60^\circ$ the effects are 30.3%, 29.1% and 37.7%, respectively, in FG-II type conical shells the effects are 31.7%, 45.8% and 64.9%, respectively.

According to the variations of the semi-vertex angle γ, comparing the values of critical dimensionless time parameter of full metal conical shells with the values for FG conical shells, the largest effect is observed at inverse quadratic case and the least effect is observed at quadratic case. At inverse quadratic case; in FG-I type conical shells, for $\gamma = 30^\circ, 45^\circ, 60^\circ$ the effects are 23.9%, 29.9% and 38.3%, respectively; in FG-II type conical shells the effects are 20.3%, 23% and 18.6%, respectively. At quadratic case; in FG-I type conical shells, for $\gamma = 30^\circ, 45^\circ, 60^\circ$ the effects are 13.3%, 15.3% and 20.6%, respectively; in FG-II type conical shells the effects are 7.4%, 8.7% and 2.5%, respectively.

In Table 9, variations of values of critical dimensionless static axial load, critical dimensionless time parameter and corresponding wavenumbers for homogeneous, FG-I type and FG-II type conical shells composed of Si_3N_4/Ni and ZrO_2 /Ti–6Al–4V with different compositional profiles and ratio R_2/h are presented.

Table 8
Variations of the values of critical dimensionless static axial load, critical dimensionless time parameter and wave numbers for homogeneous, FG-I and FG-II type conical shells with different compositional profiles and semi vertex angle γ ($N_0 = 1 \times 10^9$ N/m × s, $R_2/h = 400$; $L = 0.25 \times R_2 \sin\gamma$)

γ	$\bar{N}_{cr}^{st} \times 10^3$	$(m,n)_{cr}^{st}$	$\bar{N}_{cr}^{st} \times 10^3$	$(m,n)_{cr}^{st}$	$\bar{t}_{cr}$	n_{cr}^{din}	$\bar{t}_{cr}$	n_{cr}^{din}
Si_3N_4/Ni								
	Linear		Quadratic		Linear		Quadratic	
30°	1.013	(1, 15)	0.952	(1, 15)	2.862	18	3.125	18
45°	0.851	(1, 15)	0.800	(1, 15)	3.290	17	3.628	17
60°	0.617	(1, 12)	0.579	(1, 12)	4.449	16	5.058	16
	Cubic		Inverse quad.		Cubic		Inverse quad.	
30°	1.009	(1, 15)	1.074	(1, 15)	2.901	18	2.742	18
45°	0.848	(1, 15)	0.902	(1, 15)	3.299	17	3.003	17
60°	0.615	(1, 12)	0.654	(1, 12)	4.464	16	3.931	16
	Si_3N_4		Ni		Si_3N_4		Ni	
30°	1.326	(1, 15)	0.871	(1, 15)	2.104	18	3.603	18
45°	1.114	(1, 15)	0.732	(1, 15)	2.326	17	4.284	17
60°	0.808	(1, 12)	0.530	(1, 12)	2.854	16	6.370	16
ZrO_2 /Ti–6Al–4V								
	Linear		Quadratic		Linear		Quadratic	
30°	0.749	(1, 15)	0.703	(1, 15)	3.868	22	4.182	22
45°	0.630	(1, 15)	0.591	(1, 15)	4.613	21	5.046	21
60°	0.456	(1, 12)	0.428	(1, 12)	7.356	20	7.442	20
	Cubic		Inverse quad.		Cubic		Inverse quad.	
30°	0.746	(1, 15)	0.795	(1, 15)	3.882	22	3.601	22
45°	0.627	(1, 15)	0.668	(1, 15)	4.636	21	4.257	21
60°	0.454	(1, 12)	0.485	(1, 12)	7.384	20	6.215	20
	ZrO_2		Ti–6Al–4V		ZrO_2		Ti–6Al–4V	
30°	1.344	(1, 15)	0.675	(1, 15)	2.734	19	4.516	22
45°	1.130	(1, 15)	0.567	(1, 15)	2.919	18	5.528	21
60°	0.818	(1, 12)	0.411	(1, 12)	3.769	17	7.630	20

When the ratio R_2/h is increased, the value of the critical dimensionless static axial load are decreased, but the value of critical dimensionless time parameter, the wavenumbers corresponding to critical static axial load and the dynamic wavenumbers are increased. When the ratio R_2/h is increased the value of the critical dimensionless time parameter and dynamic wavenumbers increase quickly.

According to the variations of the ratio R_2/h, comparing the value of critical dimensionless time parameter of full ceramic conical shells with the value for FG conical shells, the largest effect is observed at quadratic case and the least effect is observed at inverse quadratic case. At quadratic case; in FG-I type conical shells, for $R_2/h = 200$; 400; 600 the effects are 29.8%, 56% and 83.3%; respectively; in FG-II type conical shells the effects are 54.9%, 72.9% and 79.5%, respectively. At inverse quadratic case; in FG-I type conical shells, for $R_2/h = 200$; 400; 600 the effects are 14.5, 29.1 and 38.2%, respectively, in FG-II type conical shells the effects are 34.4, 45.8 and 68.4%, respectively.

According to the variations of the R_2/h, comparing the value of critical dimensionless time parameter of full metal conical shells with the value for FG conical shells, the largest effect is seen at inverse quadratic case and the least effect is seen at quadratic case. At inverse quadratic case; in FG-I type conical shells, for $R_2/h = 200$, 400, 600, the effects are 19.5%, 29.9% and 38.2%, respectively; in FG-II type conical shells the effects are

Table 9
Variations of the values of critical dimensionless static axial load, critical dimensionless time parameter and wave numbers for homogeneous, FG-I and FG-II type conical shells with different compositional profiles and ratio R_2/h ($N_0 = 1 \times 10^9$ N/m × s, $\gamma = 45^\circ$, $L = 0.25 \times R_2 \sin\gamma$)

R_2/h	$\bar{N}_{cr}^{st} \times 10^3$	$(m,n)_{cr}^{st}$	$\bar{N}_{cr}^{st} \times 10^3$	$(m,n)_{cr}^{st}$	$\bar{t}_{cr}$	n_{cr}^{din}	$\bar{t}_{cr}$	n_{cr}^{din}
Si_3N_4 /Ni								
	Linear		Quadratic		Linear		Quadratic	
200	1.694	(1, 8)	1.591	(1, 8)	1.840	14	1.930	14
400	0.851	(1, 15)	0.800	(1, 15)	3.290	17	3.628	17
600	0.568	(1, 18)	0.534	(1, 18)	5.122	23	5.925	23
	Cubic		Inverse quad.		Cubic		Inverse quad.	
200	1.688	(1, 8)	1.797	(1, 8)	1.840	14	1.702	14
400	0.848	(1, 15)	0.902	(1, 15)	3.299	17	3.003	17
600	0.566	(1, 18)	0.602	(1, 18)	5.141	23	4.467	23
	Si_3N_4		Ni		Si_3N_4		Ni	
200	2.219	(1, 8)	1.455	(1, 8)	1.487	13	2.113	14
400	1.114	(1, 15)	0.732	(1, 15)	2.326	17	4.284	17
600	0.744	(1, 18)	0.488	(1, 18)	3.232	21	7.457	23
ZrO_2 /Ti–6Al–4V								
	Linear		Quadratic		Linear		Quadratic	
200	1.253	(1, 8)	1.175	(1, 8)	2.461	14	2.613	15
400	0.630	(1, 15)	0.591	(1, 15)	4.613	21	5.046	21
600	0.420	(1, 18)	0.394	(1, 18)	7.582	28	7.947	28
	Cubic		Inverse quad.		Cubic		Inverse quad.	
200	1.248	(1, 8)	1.331	(1, 8)	2.473	14	2.268	14
400	0.627	(1, 15)	0.668	(1, 15)	4.636	21	4.257	21
600	0.419	(1, 18)	0.446	(1, 18)	7.590	28	7.455	28
	ZrO_2		Ti–6Al–4V		ZrO_2		Ti–6Al–4V	
200	2.248	(1, 8)	1.128	(1, 8)	1.687	15	2.733	14
400	1.130	(1, 15)	0.567	(1, 15)	2.919	18	5.528	21
600	0.754	(1, 18)	0.378	(1, 18)	4.428	23	8.385	28

17%, 23% and 11.1%, respectively. At quadratic case; in FG-I conical type shells, for $R_2/h = 200, 400, 600$ the effects are 8.7%, 15.3% and 20.5%, respectively; in FG-II type conical shells the effects are 4.4%, 8.7% and 5.2%, respectively.

For all cases, when the compositional profile changes linearly and cubic, the values of critical dimensionless static axial load and critical dimensionless time parameter are nearly the same (see Tables 6–9).

6. Conclusions

The buckling of functionally graded truncated conical shells subjected to axial compressive load varying as a linear function of time is studied. The material properties of FG shell are varied in a state of arbitrary law distribution along the thickness. Galerkin and Runge–Kutta methods and Wolmir criterion are applied to determine the critical parameters. The results show that the values of the critical parameters are affected by the configurations of the constituent materials, compositional profile variations, loading speed variations and the variation of the shell geometry. Comparing the results of this study with those in the literature validates the present analysis.

The numerical results support the following conclusions:

(a) When the loading speed is increased, the values of the critical dimensionless time parameter and dynamic wavenumbers are increased.
(b) When semi-vertex angle γ is increased, the values of critical dimensionless static axial load, the wavenumbers corresponding to static critical axial load and the values of dynamic wavenumbers are also decreased, but the values of the critical dimensionless time parameter are increased.
(c) When the ratio R_2/h is increased, the values of the critical dimensionless static axial load are decreased, but the values of critical dimensionless time parameter, the wavenumbers corresponding to critical static axial load and the dynamic wavenumbers are increased.
(d) When the compositional profile changes quadratic, comparing the values of the critical dimensionless time parameter for full ceramic conical shells with the values of FG conical shells, the effect (as per cent) on the values of the critical dimensionless time parameter is the highest, but when compositional profile changes inverse quadratic, the effect is the lowest. Comparing with the full metal shells, it becomes opposite.
(e) Depending on the shell geometry, the longitudinal wavenumbers corresponding to minimum values of the critical axial load may not be equal to one.
(f) For all cases, when the compositional profile changes linearly and cubic, the values of critical dimensionless static axial load and critical dimensionless time parameter are nearly the same.
(g) For all compositional profiles, the values of the critical dimensionless time parameter are the highest at quadratic case and are the lowest at inverse quadratic case.
(h) For all cases, the values of critical dimensionless time parameter of FG conical shells vary between the values for full ceramic and metal conical shells.

Appendix A

Expressions A_i, B_i $(i = 1–6)$ are defined as follows:

$$A_1 = C_{11}B_1 + C_{21}B_2, \quad A_2 = C_{11}B_2 + C_{21}B_1, \quad A_3 = C_{11}B_3 + C_{21}B_4 + C_{12},$$
$$A_4 = C_{11}B_4 + C_{21}B_3 + C_{22}, \quad A_5 = C_{61}B_5, \quad A_6 = C_{61}B_6 + C_{62}, \quad B_1 = C_{10}D,$$
$$B_2 = -C_{20}D, \quad B_3 = (C_{20}C_{21} - C_{11}C_{10})D, \quad B_4 = (C_{20}C_{11} - C_{21}C_{10})D, \quad B_5 = 1/C_{60},$$
$$B_6 = C_{61}/C_{60}, \quad D = 1/\left|(C_{10})^2 - (C_{20})^2\right| \tag{A.1–A.13}$$

in which expressions C_{1k}, C_{2k} and C_{6k} $(k = 0, 1, 2)$ are defined as follows:

$$C_{1k} = h^{k+1}\int_{-0.5}^{0.5} \bar{z}^k \frac{(E_t - E_b)V_c + E_b}{1 - [(v_t - v_b)V_c + v_b]^2}\,\mathrm{d}\bar{z}, \tag{A.14.1}$$

$$C_{2k} = h^{k+1}\int_{-0.5}^{0.5} \bar{z}^k \frac{[(E_t - E_b)V_c + E_b][(v_t - v_b)V_c + v_b]}{1 - [(v_t - v_b)V_c + v_b]^2}\,\mathrm{d}\bar{z}, \tag{A.14.2}$$

$$C_{6k} = h^{k+1}\int_{-0.5}^{0.5} \bar{z}^k \frac{(E_t - E_b)V_c + E_b}{1 + (v_t - v_b)V_c + v_b}. \tag{A.14.3}$$

References

[1] M. Koizumi, The concept of FGM, *Ceramics Transactions, Functionally Gradient Materials* 34 (1993) 3–10.
[2] M. Koizumi, FGM activities in Japan, *Composites* 28 (1-2) (1997) 1–4.
[3] W. Pompe, H. Worchorch, M. Epple, W. Friess, M. Gelinsky, P. Greil, U. Hempel, D. Scharnweber, K. Schulte, Functionally graded materials for biomedical applications, *Materials Science Engineering A* 362 (1–2) (2003) 40–60.
[4] E. Müller, C. Drašar, J. Schilz, W.A. Kaysser, Functionally graded materials for sensor and energy applications, *Materials Science Engineering* A362 (1–2) (2003) 17–39.

[5] S. Suresh, A. Mortensen, *Fundamentals of Functionally Graded Materials: Processing and Thermo-Mechanical Behavior of Graded Metals and Metal-Ceramic Composites*, IOM Communications, London, 1998.
[6] Y. Miyamoto, W.A. Kaysser, B.H. Rabin, A. Kawasaki, R.G. Ford, *Functionally Graded Materials: Design*, Kluwer Academic, Boston, MA, 1999.
[7] V. Birman, Buckling of functionally graded hybrid composite plates, *Proceedings of the 10th Conference Engineering Mechanics*, Boulder, USA, 1995.
[8] C.T. Loy, J.N. Lam, J.N. Reddy, Vibration of functionally graded cylindrical shells, *International Journal of Mechanical Sciences* 41 (1999) 309–324.
[9] S.C. Pradhan, C.T. Loy, J.N. Lam, J.N. Reddy, Vibration characteristics of functionally graded cylindrical shells under various boundary conditions, *Applied Acoustics* 61 (1) (2000) 119–129.
[10] J.N. Reddy, Z.Q. Cheng, Frequency correspondence between membranes and functionally graded spherical shallow shells of polygonal plan form, *International Journal of Mechanical Sciences* 44 (5) (2002) 967–985.
[11] S. Pitakthapanaphong, E.P. Busso, Self-consistent elasto-plastic stress solutions for functionally graded material systems subjected to thermal transients, *Journal of Mechanics and Physics of Solids* 50 (2002) 695–716.
[12] J. Woo, S.A. Meguid, Thermo-mechanical post-buckling analysis of functionally graded plates and shallow cylindrical shells, *Acta Mechanica* 165 (2003) 99–115.
[13] J. Yang, H.S. Shen, Parametric resonance of shear deformable functionally graded cylindrical panels in thermal environment, *Journal of Sound and Vibration* 261 (5) (2003) 871–893.
[14] H.S. Shen, Post-buckling analysis of pressure loaded functionally graded cylindrical shells in thermal environments, *Journal of Engineering Structures* 25 (2003) 487–497.
[15] S.J. Kitipornchai, J. Yang, K.M. Liew, Semi analytical for nonlinear vibration of laminated FGM plates with geometric imperfections, *International Journal of Solids and Structures* 41 (2004) 2235–2257.
[16] W.Q. Chen, Z.G. Bian, C.F. Lv, H.J. Ding, vibration analysis of a functionally graded piezoelectric hollow cylinder filled with compressible fluid 3D, *International Journal of Solids and Structures* 41 (3-4) (2004) 947–964.
[17] B.P. Patel, M.S. Cupta, M.S. Loknath, C.P. Kadu, Free vibration analysis of a functionally graded elliptical cylindrical shells using higher-order theory, *Journal of Composite Structures* 69 (2005) 259–270.
[18] K.M. Liew, J. Yang, Y.F. Wu, Nonlinear vibration of a coating-FGM-substrate cylindrical panel subjected to a temperature gradient, *Computer Methods in Applied Mechanics and Engineering* 195 (9-12) (2006) 1007–1026.
[19] R.K. Bhangale, N. Ganesan, P. Chandramouli, Linear thermo-elastic buckling and free vibration behavior of functionally graded truncated conical shells, *Journal of Sound and Vibration* 292 (1-2) (2006) 341–371.
[20] R.K. Bhangale, N. Ganesan, Free vibration of simply supported functionally graded and layered magneto-electro-elastic plates by finite element method, *Journal of Sound and Vibration* 294 (2006) 1016–1038.
[21] P. Seide, Axisymmetrical buckling of circular cones under axial compression, *Journal of Applied Mechanics* 23 (1956) 626–628.
[22] K.M. Mushtari, A.V. Sachenkov, Stability of cylindrical and conical shells of circular cross section with simultaneous action of axial compression and external normal pressure, NASA TM-1433, 2000.
[23] L. Lackman, J. Renzien, Buckling of circular cones under axial compression, *Journal of Applied Mechanics* 27 (1960) 458–460.
[24] P. Seide, Buckling of circular cones under axial compression, *Journal of Applied Mechanics* 28 (1961) 315–326.
[25] V.I. Weingarten, E.J. Morgan, P. Seide, Elastic stability of thin walled cylindrical and conical shells under combined pressure and axial compression, *AIAA Journal* 3 (1965) 118–125.
[26] M. Baruch, O. Harari, J. Singer, Low buckling loads of axially compressed conical shells, *Journal of Applied Mechanics* 38 (1970) 384–392.
[27] J. Tani, Y. Yamaki, Buckling of truncated conical shells under axial compression, *AIAA Journal* 8 (1970) 568–570.
[28] P.E. Tovstik, Some problems of the stability of cylindrical and conical shell, *Journal of Applied Mathematics and Mechanics* 47 (1985) 657–663.
[29] L. Tong, B. Tabarrok, T.K. Wang, Simple solution for buckling of Orthotropic conical shells International, *Journal of Solids and Structures* 29 (1992) 933–946.
[30] A. Spagnoli, M.K. Chryssanthopoulos, Elastic buckling and post-buckling behaviour of widely stiffened conical shells under axial compression, *Journal of Engineering Structures* 21 (1999) 845–855.
[31] A. Spagnoli, Koiter circles in the buckling of axially compressed conical shells, *International Journal of Solids and Structures* 40 (2003) 6095–6109.
[32] Y.S. Tamura, C.D. Babcock, Dynamic stability of cylindrical shells under step loading, *Journal of Applied Mechanics* 42 (1) (1975) 190–194.
[33] G.J. Simitises, *Dynamic Stability of Suddenly Loaded Structures*, Springer, Berlin, 1990.
[34] R. Tanov, A. Tabieai, G.J. Simitises, Effect of static preloading on the dynamic buckling of laminated cylinders under sudden pressure, *Mechanics of Composites Materials and Structures* 6 (1999) 195–206.
[35] C. Bisagni, Dynamic buckling of fiber composite shells under impulsive axial compression, *Thin-Walled Structures* 43 (2005) 499–514.
[36] A.S. Volmir, *Stability of Elastic Systems*, Nauka, Moscow, 1967 (English Translation: Foreign Tech. Division, Air Force Systems Command. Wright-Patterson Air Force Base, OH, AD628508).
[37] M.A. Shumik, On the stability of a truncated conical shell subject to a dynamic axial compression, *Soviet Applied Mechanics* 6 (11) (1970) 122–126.
[38] V.V. Mitriaikin, L.U. Baktieva, Investigation of the stability of circular conical shells subjected to dynamic loading, Kazan State University, Russian, *Actual Problems of Mechanics of Shells* 24 (1985) 186–191.

[39] V.L. Agamirov, A.A. Solomonenko, Stability of conical shells subjected to a dynamic axial compression, VIINITI DEP., No. 1136-B, Moscow, 1987, pp. 1–12 (in Russian).
[40] V.L. Agamirov, *Dynamic Problems of Nonlinear Shells Theory*, Nauka, Moscow, 1990 (in Russian).
[41] A.N. Yakushev, The stability of orthotropic conical shells subjected to a dynamic loading, *Research on the Theory of Plates and Shells, Kazan State University, Russian* (24) (1991) 186–191.
[42] A.H. Sofiyev, O. Aksogan, Buckling of a conical thin shell with variable thickness under a dynamic loading, *Journal of Sound and Vibration* 13 (3) (2003) 329–343.
[43] G.H. Praveen, J.N. Reddy, Nonlinear transient thermal elastic analysis of functionally graded ceramic–metal plates, *International Journal of Solids and Structures* 35 (33) (1998) 4457–4476.
[44] J.N. Reddy, C.D. Chin, Thermal-mechanical analysis of functionally graded cylinders and plates, *Journal of Thermal Stresses* 21 (1998) 593–626.
[45] J.N. Reddy, Analysis of functionally graded plates, *International Journal for Numerical Methods in Engineering* 35 (33) (2000) 4457–4476.
[46] T.Y. NG, K.Y. Lam, K.M. LIEW, J.N. Reddy, Dynamic stability analysis of functionally graded cylindrical shells under periodic axial loading, *International Journal of Solids and Structures* 38 (2001) 1295–1309.
[47] J. Yang, H.S. Shen, Dynamic response of initially stressed functionally graded rectangular thin plates, *Journal of Composite Structures* 54 (2001) 497–508.
[48] K.M. Liew, X.Q. HE, T.Y. NG, S. Kitipornchai, Active control of FGM shell subjected to a temperature gradient via piezoelectric sensor/actuator patches, *International Journal for Numerical Methods in Engineering* 55 (2002) 653–668.
[49] X.Q. HE, K.M. Liew, T.Y. NG, A. Sivashanker, A FEM model for the active control of curved FGM shells using piezoelectric sensor/actuator layers, *International Journal for Numerical Methods in Engineering* 54 (6) (2002) 853–870.
[50] T.Y. NG, X.Q. HE, K.M. Liew, Finite element modeling of active control of functionally graded shells in frequency domain via piezoelectric sensors and actuators, *Computational Mechanics* 28 (1) (2002) 1–9.
[51] S.S. Vel, R.C. Batra, Three-dimensional analysis of transient thermal stresses in functionally graded rectangular plates, *International Journal for Numerical Methods in Engineering* 40 (25) (2003) 7181–7196.
[52] A.H. Sofiyev, E. Schnack, The stability of functionally graded cylindrical shells under linearly increasing dynamic torsional loading, *Journal of Engineering Structures* 26 (10) (2004) 1321–1331.
[53] A.H. Sofiyev, The stability of functionally graded truncated conical shells subjected to a-periodic impulsive loading, *International Journal of Solids and Structures* 41 (13) (2004) 3411–3424.
[54] A.H. Sofiyev, The stability of compositionally graded ceramic-metal cylindrical shells under a-periodic axial impulsive loading, *Journal of Composite Structures* 69 (2005) 257–267.
[55] T. Kubiak, Dynamic buckling of thin-walled composite plates with varying widthwise material properties, *International Journal of Solids and Structures* 42 (2005) 5555–5567.
[56] A. Tylikowsky, Dynamic stability of functionally graded plate under in-plane compression, *Mathematical Problems in Engineering* 4 (2005) 411–424.
[57] J. Zhu, C. Chen, Y.P. Shen, S.L. Wang, Dynamic stability of functionally graded piezoelectric circular cylindrical shells, *Materials Letters* 59 (2005) 477–485.
[58] L. Wu, H. Wang, D. Wang, Dynamic stability analysis of FGM plates by the moving least squares differential quadrature method, *Journal of Composite Structures* (2005), in press.
[59] M. Ganapathi, Dynamic stability characteristics of functionally graded materials shallow spherical shells, *Journal of Composite Structures* (2006), in press.
[60] S.Y. Lu, L.K. Chang, Thermal buckling of conical shells, *AIAA Journal* 5 (10) (1967) 1877–1882.
[61] R.M. Jones, H.S. Morgan, Buckling and vibration of cross-ply laminated circular cylindrical shells, *AIAA Journal* 13 (1975) 664–671.
[62] S.H. Shen, Postbuckling analysis of stiffened laminated cylindrical shells under combined external liquid pressure and axial compression, *Engineering Structures* 20 (8) (1997) 738–751.
[63] S.H. Shen, Q.S. Li, Postbuckling of cross-ply laminated cylindrical shells with piezoelectric actuators under complex loading conditions, *International Journal of Mechanical Sciences* 44 (2002) 1731–1754.
[64] Y.S. Touloukian, *Thermo Physical Properties of High Temperature Solid Materials*, McMillan, New York, 1967.